Review

Carbon Future

The future of carbon anodes for lithium-ion batteries: The rational regulation of graphite interphase

Bin Cao[1,2], Mengjiao Du[2], Zirong Guo[2], Huan Liu[2], Chong Yan[3], Aibing Chen[4], Xiang Chen[1,5], Cheng Tang[1,6]✉, Jia-Qi Huang[3]✉, and Qiang Zhang[1,6,7,8]✉

[1] *Tsinghua Center for Green Chemical Engineering Electrification, Beijing Key Laboratory of Green Chemical Reaction Engineering and Technology, Department of Chemical Engineering, Tsinghua University, Beijing 100084, China*
[2] *College of Materials Science and Engineering, Xi'an University of Science and Technology, Xi'an 710054, China*
[3] *Advanced Research Institute of Multidisciplinary Science, School of Materials Science and Engineering, Beijing Institute of Technology, Beijing 100081, China*
[4] *College of Chemical and Pharmaceutical Engineering, Hebei University of Science and Technology, Shijiazhuang 050018, China*
[5] *School of Chemical Engineering, Sungkyunkwan University (SKKU), 2066, Seoburo, Jangan-gu, Suwon 440-746, Republic of Korea*
[6] *Institute for Carbon Neutrality, Tsinghua University, Beijing 100084, China*
[7] *Shanxi Research Institute for Clean Energy, Tsinghua University, Taiyuan 030032, China*
[8] *Ordos Laboratory, Ordos 017010, China*

Cite This: *Carbon Future* **2024**, *1*, 9200017

Read Online

ABSTRACT: Interphase regulation of graphite anodes is indispensable for augmenting the performance of lithium-ion batteries (LIBs). The resulting solid electrolyte interphase (SEI) is crucial in ensuring anode stability, electrolyte compatibility, and efficient charge transfer kinetics, which in turn dictates the cyclability, fast-charging capability, temperature tolerance, and safety of carbon anodes. Continuous research endeavors are deepening our comprehension of the interphasial chemistry, underscoring the imperative to refine the SEI through economically viable and scalable techniques. The ongoing advancement of surface coating techniques involving amorphous carbons or Li-ion conductors, along with electrolyte formulations optimization such as the integration of film-forming additives, has become the cornerstones in regulating the SEI. These innovations are reshaping the landscape of current LIBs by refining the electrode interphase, paving the way to construct more potent and efficient energy storage systems. The relentless drive to optimize the interphase through cutting-edge technologies is central to the future of LIBs, with the ambitious goals of achieving higher energy densities, ensuring safety, and promoting sustainability in energy storage solutions. This review affords a comprehensive overview of the progression in carbon anode development and current status of their industrialization, underscoring the critical role of interphase regulation engineering in advancing the LIB technology.

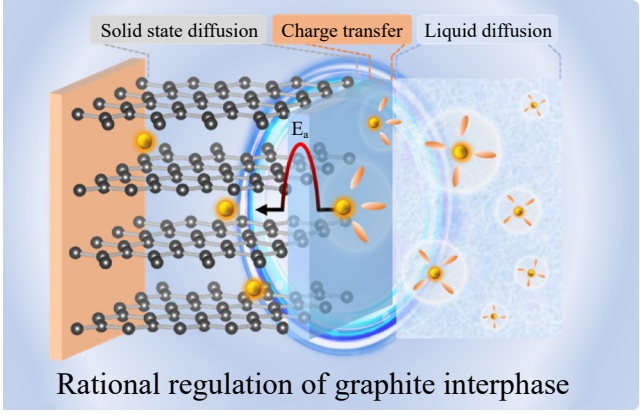

KEYWORDS: graphite anode, solid electrolyte interphase, Li-ion batteries, surface coating, electrode−electrolyte interface regulation, fast-charging carbon anode

1 Introduction

The first commercial rechargeable lithium batteries (Li-MoS_2) proposed by *Moli Energy* in 1987 exhibited an insurmountable safety problem due to the formation of lithium dendrites which cause short-circuiting. This vital issue has promoted researchers to find a more suitable anode instead of lithium anode for addressing the safety risk and unsatisfied calendar life. $LiCoO_2$ and $LiMn_2O_4$ cathodes with high lithium storage potentials > 4.0 V vs. Li^+/Li (the following potentials are all referred to Li^+/Li, if there is no other statement) were found in 1980[1] and 1984[2], respectively; however, their application in rechargeable lithium batteries was hindered at that time, primarily due to the absence of compatible anodes and suitable electrolytes. The electrolytes of that era contained ethers as co-solvents to stabilize lithium anodes and are not stable above 4.0 V. In 1991, the birth of commercial Li-ion batteries (LIBs) was

Received: July 26, 2024; **Revised:** August 27, 2024
Accepted: September 9, 2024

✉Address correspondence to Cheng Tang, chengnet0@tsinghua.edu.cn; Jia-Qi Huang, jqhuang@bit.edu.cn; Qiang Zhang, zhang-qiang@mails.tsinghua.edu.cn

https://doi.org/10.26599/CF.2024.9200017

promoted by *Sony* using petroleum coke as the amorphous carbon anode and $LiCoO_2$ as the high-energy cathode. They functioned as hosts for the transfer of Li^+ ions between the anode and cathode, playing a critical role in establishing the "rocking chair" mechanism that characterizes Li-ion secondary batteries. The selection of carbonaceous anodes initially paved the way due to their high compatibility with electrolytes and ability to efficiently insert lithium at a lower potential region (< 1.0 V), thus enabling the practical application and commercialization of LIBs[3].

Graphite, currently the predominant anodes applied in LIBs with a near-monopoly market share of 98%[4], was not originally used in the first generation of these batteries. Although the electrochemical intercalation of Li^+ ions into graphite[5] to form LiC_6, the first stage of lithium-graphite intercalation compound (Li-GIC), was described as early as 1983, its widespread adoption was delayed due to compatibility issue with the electrolyte of the time. In the early days of LIBs development, propylene carbonate (PC) was the favored co-solvent for electrolytes due to its robust solvation ability, broad liquid range (from −49 to 242 °C), and high voltage stability (> 4.0 V). However, the co-intercalation of PC-solvated Li^+ ions caused severe structural damage, known as exfoliation, to the graphite anode before a stable electrode interphase could form. This issue significantly postponed the adoption of graphite as the anode materials in LIBs. The tide began to turn with the discovery by Dahn and co-workers that ethylene carbonate (EC) was crucial for forming a protective layer, known as the solid electrolyte interphase (SEI), on the surface of graphite anodes[6]. This SEI layer allowed for reversible intercalation and deintercalation of Li^+ ions within the graphite's layered structure, sparking a new focus on the interphasial chemistry of electrode materials. The graphite anodes are highly sensitive to the electrolyte composition, and the formation of a well-structured SEI is essential for achieving high Coulombic efficiency and stable cycling performance. The use of EC in combination with linear carbonates, such as dimethyl carbonate (DMC) and diethylene carbonate (DEC), has been well demonstrated to provide optimal electrolyte formulations. This mixture enables graphite anodes to demonstrate high initial Coulombic efficiency (ICE, > 90%) and reliable cycle life. Compared to amorphous carbon anodes, graphite anodes offer an average low delithiation potential (~ 0.15 V), high ICE, and a reversible capacity in the range of 320 to 360 $mAh{\cdot}g^{-1}$. These characteristics are conducive to achieving greater energy density in LIBs. The synergy between EC-centric electrolytes and graphite anodes has since led to a 30–50% increase in the energy density of LIBs[7], marking a new era for the application of these materials in electrochemical energy fields.

Drawing from the evolutionary journey of graphite anode utilization in LIBs, a paramount aspect is the establishment of a robust SEI during the battery's initial preconditioning stage. This SEI formation is not only fundamental to the successful integration of graphite anodes into LIBs but also crucial for optimizing their electrochemical performances, including metrics such as energy and power densities, as well as cyclability. Despite the seemingly minute components that constitute the SEI in LIBs, their impact on the overall battery performance is substantial. The SEI plays a multifaceted role by bolstering electrochemical stability, affecting the transport of ions at the interphase and the associated impedance, guiding the design of electrode materials, and acting as a diagnostic tool for battery health[8]. The pursuit of deeper insights into the properties of SEI and its dynamic behavior is essential for propelling battery technology forward, steering it towards safer, more efficient, and longer-lasting energy storage systems. The focus on the interface regulation engineering of graphite anodes has gained significant attention due to its potential to substantially improve electrochemical performance (Fig. 1a). This approach is promising for pushing the boundaries of LIB performance, transcending traditional limitations, and setting the stage for devices that are more efficient, powerful, and enduring. In this concise Review, we encapsulate the trajectory and transformation of interphase regulation engineering for graphite anodes within LIBs (Fig. 1b).

In this contribution, we delve into the lithium storage mechanisms, explore various interfacial characterization techniques, and discuss strategies for interphase regulation. Our emphasis is on the latest advancements in the field of interface regulation engineering, which are crucial for the continued enhancement and innovation of LIBs technology.

2 The lithium storage mechanism of graphite anodes

The crystalline structure of graphite anode is a layered arrangement of graphene sheets stacked upon one another. Each sheet is a lattice of carbon atoms arranged hexagonally, with sp^2 hybridization, and the sheets are held together by van der Waals forces (Fig. 2a). Since the layered structure of graphite is slidable due to the weak interlayer interaction (van der Waals forces), the structure integrity is critical to impact the reversibility of lithium storage. Typically, graphite particles exhibit two types of surfaces: basal and edge planes, with the edge planes being more chemically reactive than the basal planes. Edge planes are the primary sites for lithium intercalation and deintercalation[9], where electrolyte decomposition, SEI formation, and exfoliation predominantly occur. For fresh graphite electrodes, a SEI layer consisted of inorganic species (LiF, Li_2CO_3, Li_2O, LiN_xO_y, and so on) and organic species (lithium alkyl carbonates, and so on) is formed on the graphite surface at approximately 0.9 V, a result of the reductive decomposition of electrolytes[10]. The formation of SEI is irreversible, leading to an initial capacity loss. The well-formed SEI is electronically insulating but allows for the diffusion of Li ions, which helps to prevent further electrolyte decomposition during subsequent lithium intercalation. With further lithium intercalating into the graphite hosts, the formation of Li-GICs exhibits a staging phenomenon due to the periodic intercalating of lithium layers between the graphene sheets[11]. As illustrated in Fig. 2b, the highest stage (1-stage) of Li-GICs with the stoichiometry LiC_6 is formed at full lithiation state, offering a theoretical capacity of 372 $mAh{\cdot}g^{-1}$ (850 $mAh{\cdot}cm^{-3}$). The overall lithium storage behavior of graphite anodes is characterized by a long, flat low-voltage plateau, low voltage gap, and a high ICE value. These features are highly advantageous for achieving high energy efficiency and delivering a high operating voltage, realizing rechargeable LIBs with higher energy densities. The pathway for Li ion diffusion from the electrolyte into the interlayers of graphite is depicted in Fig. 2c. Initially, the slow solid-state diffusion of Li within the graphite interlayers was considered the rate-determining step[12], affecting the charging rate. However, the charge transfer step is now widely accepted as the rate-determining step for Li intercalation into graphite[8, 13]. Consequently, the regulation of the interphase has become a critical aspect in facilitating rapid Li intercalation into graphite anodes.

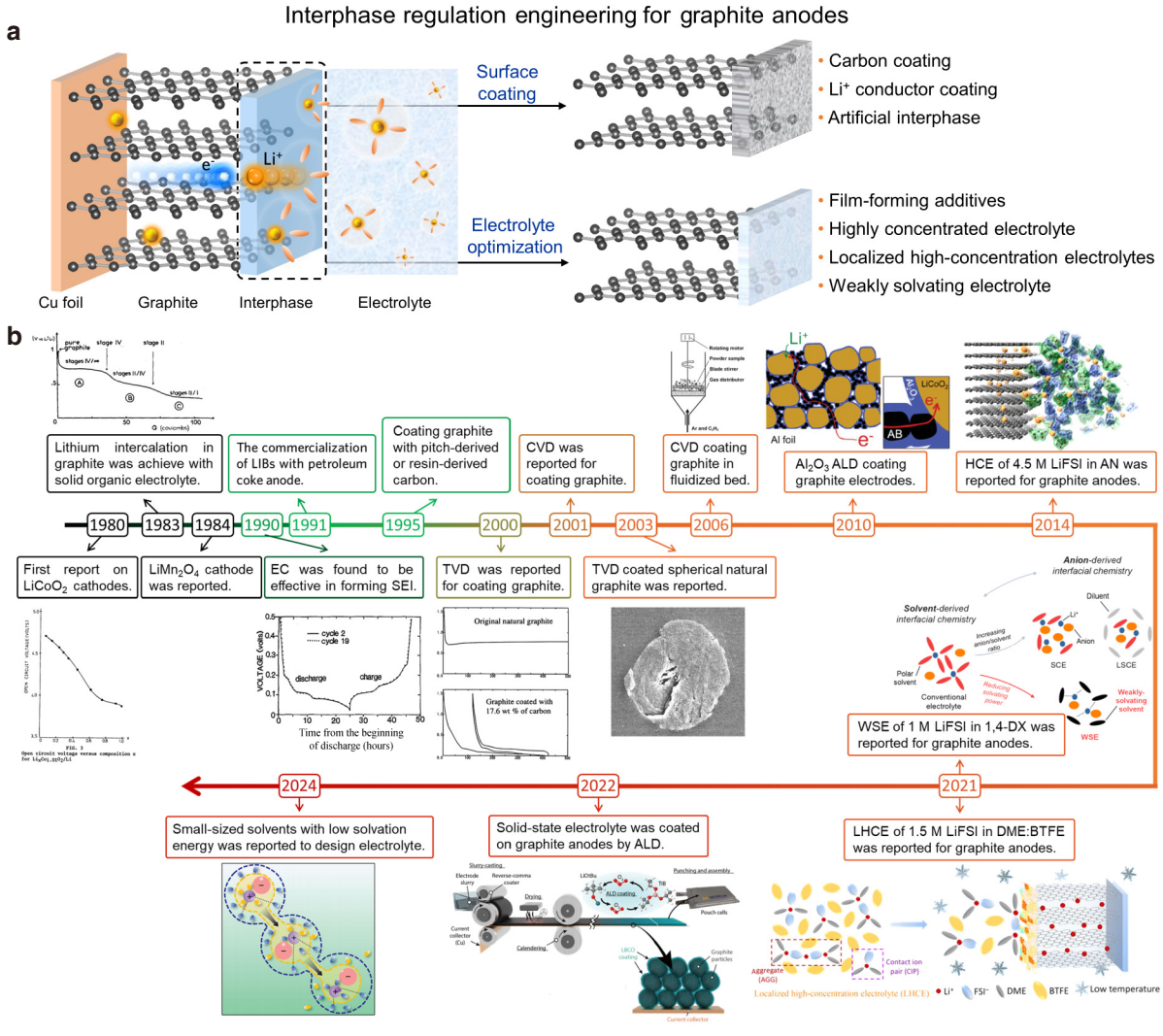

Fig. 1. Interphase regulation engineering of graphite anodes and its development. a, Schematic for the concept of interphase regulation engineering for graphite anodes. **b,** Timeline of the development of graphite anodes for lithium storage. Reproduced with permission from Ref.[1, 2, 5, 6, 29–33, 36, 37, 51, 53, 55, 56], © Elsevier Ltd. 1980; © Elsevier Ltd. 1984; © Elsevier B.V. 1983; © The Electrochemical Society, Inc. 1990; © Elsevier Science S.A. 1995; © Elsevier Science Ltd. 2001; © The Electrochemical Society 2000; © WILEY-VCH Verlag GmbH & Co. KGaA, Weinheim 2023; © Elsevier Ltd. 2026; © WILEY-VCH Verlag GmbH & Co. KGaA, Weinheim 2010; © Wiley-VCH GmbH 2021; © American Chemical Society 2014; © Wiley-VCH GmbH 2020; © Wiley-VCH GmbH 2020; and © Lu, D. et al. 2024.

3 Interphase characterization

Characterizing the interphase of graphite anodes (Fig. 3a) is essential for elucidating the correlation between interfacial structure and lithium storage performance. X-ray photoelectron spectroscopy (XPS), a potent surface-sensitive analytical tool, facilitates the examination of the chemical composition, oxidation states of elements, and electronic configurations of materials. XPS has been widely applied to the analysis of both surface layers[14, 15] and the SEI of graphite[16] (Fig. 3b). XPS identifies pivotal constituents, including inorganic species, organic compounds, doping heteroatoms, and lithium salts, thereby elucidating the chemical composition of surface coating layers as well as the structural characteristics and formation mechanisms of the SEI[17, 18].

Furthermore, time-of-flight secondary ion mass spectrometry (TOF-SIMS) enables the three-dimensional characterization of chemical composition with depth profiling and high spatial resolution. The combined use of TOF-SIMS and scanning electron microscopy (SEM) leverages the strengths of both techniques, providing high-resolution imaging and precise chemical characterization, which is powerful for surface analysis (Fig. 3c)[19, 20]. Both XPS and TOF-SIMS provide an average representation of the chemical information at the graphite surface, while the chemical composition on the basal and edge planes can exhibit distinct properties due to graphite's anisotropic nature, a factor often overlooked. Fourier transform-infrared spectroscopy (FT-IR) is frequently utilized to analyze functional groups, thereby inferring the molecular structures of organic species within the coating layer or SEI, and contributing to the understanding of the surface layer's composition and functionality (Fig. 3d)[18].

Additionally, both SEM and transmission electron microscopy (TEM) provide detailed insights into the nanoscale structure of the coating layer and SEI, including composition, crystal structure, thickness, and their interactions with graphite particles (Fig. 3e and 3f). Noteworthily, certain species within the SEI and lithiated graphite are highly sensitive to the electron beam, as high-energy exposure can lead to irradiation damage or delithiation. To address

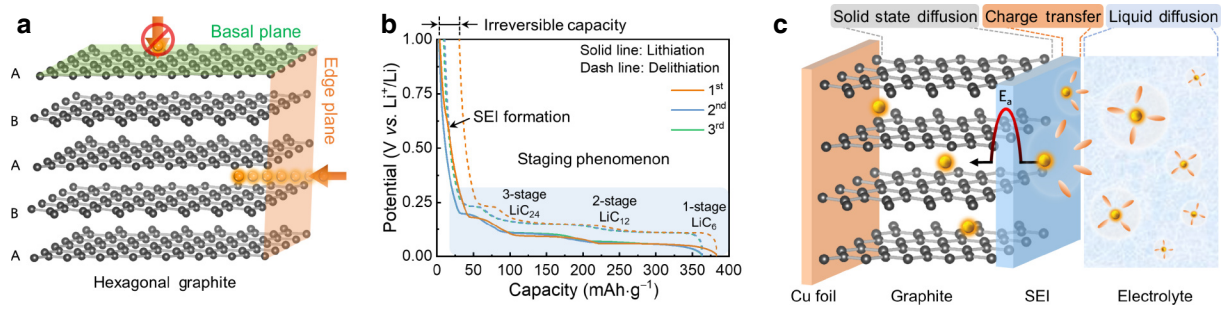

Fig. 2. The layered structure and lithium storage mechanism of graphite. a, Schematic of the typical layered structure of hexagonal graphite with ABAB… staking and space group of P63/mmc. **b**, The voltage profile of graphite during lithium storage. **c**, Li^+ diffusion path from electrolyte into the layered structure of graphite anodes.

this issue, cryo-transmission electron microscopy (cryo-TEM)[21, 22], which operates at cryogenic temperatures, is employed as an alternative to conventional TEM. Cryo-TEM is especially advantageous for examining sensitive and beam-sensitive materials, including the SEI, which often degrades under standard TEM conditions. Employing cryo-TEM facilitates the nanoscale investigation of the SEI's composition and structure on graphite (Fig. 3g) without compromising the target's inherent structure[23]. The integration and judicious application of these characterization techniques can elucidate the intricate interplay among electrode materials, the coating layer, electrolytes, and the SEI.

In addition, electrochemical impedance spectro-scopy (EIS) is a powerful electrochemical technique[24] for characterizing the interphase between graphite and electrolytes. The Nyquist plots obtained from EIS measurements help to elucidate various interfacial electrochemical phenomena, such as the characteristics of the SEI[25], charge transfer resistance[19], lithium-ion diffusion kinetics and lithium plating[26], which are critical in determining cycling stability and rate capability. For graphite anodes, it is desirable to perform EIS measurements in three-electrode cells or symmetrical cells to avoid interference from lithium electrodes. Based on the EIS results, employing the concept of distribution of relaxation time (DRT)[27] is helpful to decouple and quantify intertwined electrochemical lithium transfer kinetics in time dimensions, such as interfacial properties, charge transfer, and ion diffusion[16] (Fig. 3h). These non-destructive techniques offer a deep understanding by probing the intricacies of the graphite electrode interface, facilitating advancements in LIBs through a profound understanding of electrode interfacial phenomena.

4 Surface coating for electrode interphase regulation

Surface coating methods are strongly considered to fabricate a protective barrier as the functional electrode interface of graphite anodes. This engineered interface aims to preclude direct electrolyte contact, thereby fostering the formation of a more uniform and stable SEI. Alternatively, it can act as an artificial interphase that circumvents SEI formation entirely, thereby averting further electrolyte decomposition. This approach not only accelerates Li^+ transfer but also enhances Coulombic efficiency and mitigates irreversible capacity loss. Various layers have been investigated for coating the surface of graphite anodes, such as amorphous carbons, Li^+ conductors, metal oxides, and polymers. The methodologies for applying these coatings encompass a range of techniques such as pyrolysis of organic precursor layers, the sol–gel process, chemical vapor deposition (CVD), wet-coating, atomic layer deposition (ALD), thermal vapor decomposition (TVD) and other sophisticated treatment processes (Fig. 1b). Both carbon and Li^+ conductor coatings are recognized as the most efficacious strategies for establishing a functional electrode interphase and enhancing the electrochemical performance of graphite anodes. In the subsequent sections, we concentrate our discussion on these two aspects, delving into their specific contributions and mechanisms in regulating the electrode interphase to boost lithium storage performance.

4.1 Carbon coating

The application of carbon coatings on graphite anode surfaces represents a highly efficacious strategy for augmenting anode performance. This method entails the deposition of a thin carbonaceous layer on graphite particles, which serves to stabilize the electrode–electrolyte interface and bolster the overall electrochemical performance of graphite anodes[28]. In 1995, Kuribayashi and co-workers discovered that anodes coated with carbon layers derived from pitches or resins demonstrated enhanced lithium storage stability and superior reversible capacity[29]. The irreversible capacity of graphite anodes was notably diminished through CVD coating, attributed to the formation of a compact and thin SEI on graphite anodes (Fig. 4a)[30]. Additionally, Yoshio et al. reported that TVD carbon-coated natural graphite[31] exhibited diminished sensitivity to electrolytes compared to uncoated counterparts (Fig. 4b). The TVD process is essentially a variant of the CVD technique, involving the deposition of a carbon layer through the gas-phase carbonization of a precursor. In a PC-based electrolyte, spherical carbon-coated natural graphite exhibited a high Coulombic efficiency exceeding 92%, facilitated by a 6 wt% carbon coating through the TVD (Fig. 4c)[32]. Chen and co-workers[33] further improved the uniformity of the coating by employing CVD within a fluidized bed reactor to coat natural graphite spheres with pyrolytic carbon. The ICE and cyclability were markedly enhanced for the coated graphite, which were attributed to the reduced specific surface area. The formation of an internal SEI was inhibited, while a thin, compact SEI was formed on the outer surface (Fig. 4d). The construction of an ultrathin turbostratic carbon coating layer has been validated for its efficacy in enhancing the fast-charging capability of graphite anodes[34]. The turbostratic carbon layer was revealed to supply a plethora of active sites and create expedited pathways for Li^+ diffusion. Furthermore, the application of a soft carbon coating on the surface of graphite anodes has been identified as an effective strategy to mitigate the formation of resistive films[35]. This intervention facilitates charge transfer and reduces the energy barrier, thereby enhancing cyclability and fast-charging capabilities.

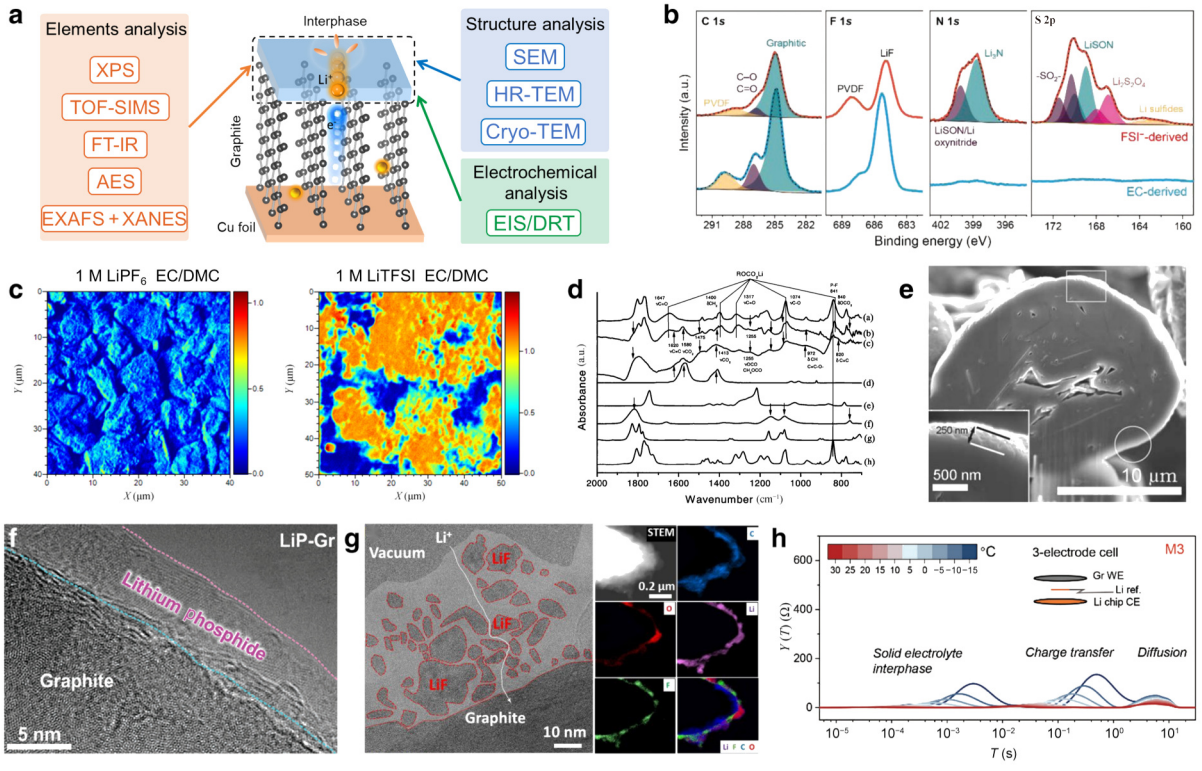

Fig. 3. Characterization methods for interphase of graphite anodes. a, Commonly used interphase characterization methods. **b**, XPS analyzing the components in SEI with different electrolyte. Reproduced with permission from Ref.[16], © Wiley-VCH GmbH 2022. **c**, TOF-SIMS mapping revealing the Li plating situation on the surface of graphite anodes. Reproduced with permission from Ref.[19], © Wiley-VCH GmbH 2022. **d**, FT-IR showing the functional groups in SEI[18], © Ota, H. et al, 2004 **e**, SEM images of focused-ion beam cross-section showing coating layer on the graphite particles for carbon coating layer. Reproduced with permission from Ref.[33], © Elsevier Ltd. 2026. **f**, High-resolution TEM (HR-TEM) image characterizing the Li_3P interphase on the surface of graphite anodes. Reproduced with permission from Ref.[14], © Wiley-VCH GmbH 2023. **g**, Cryo-TEM image with corresponding high-angle annular dark-field scanning transmission electron microscopy (HAADF STEM) image and electron energy loss spectroscopy (EELS) mapping, revealing the structure and composition of SEI on graphite anodes with FEC film-forming additive. Reproduced with permission from Ref.[23], © The Royal Society of Chemistry 2021. **h**, DRT analysis of the Nyquist plot of graphite anodes at different temperatures for decoupling the intertwined electrochemical steps. Reproduced with permission from Ref.[16], © Wiley-VCH GmbH 2022.

Despite the considerable enhancements afforded by carbon coatings, several challenges remain. Firstly, achieving a uniformly coated layer is imperative for consistent performance but presents significant difficulties, particularly in large-scale manufacturing processes. Secondly, the thickness of the coating layer necessitates optimization to reconcile improvements in electrolyte compatibility with material properties, as the low density and lithium storage capacity of the amorphous carbon coating layer can diminish the electrode density and reversible capacity. Lastly, the development of a scalable, cost-effective coating technology with streamlined procedures is vital for the industrial viability of this strategy. Future research endeavors should concentrate on surmounting these hurdles by employing advanced, controllable carbon coating technologies that ensure uniformity, optimize coating thickness, and are both scalable and economically viable.

4.2 Li-ion conductor coating

The formation of SEI that is conductive to Li ions but insulating to electrons is a critical factor in affecting the performance of graphite anodes. To this end, Li^+ conductor materials are ideal for creating an artificial interphase on the anode surface.

For example, an ultrathin layer of Al_2O_3 was meticulously applied to graphite electrodes through ALD method, which can effectively curb undesirable electrolyte decomposition reactions[36]. This ultrathin Al_2O_3-coated natural graphite has demonstrated remarkable compatibility with PC, enhanced cycling performance at elevated temperatures (Fig. 4e), and improved safety due to the high stability and minimal kinetic hindrance of the ultrathin Al_2O_3 layer. An innovative application of ALD involved the coating of a single-ion conducting solid-state electrolyte, Li_3BO_3-Li_2CO_3 (LBCO), as an artificial SEI on post-calendared graphite electrodes[37]. With an optimal LBCO coating thickness of 20 nm, these graphite anodes have achieved a significant capacity retention of 80% after 500 cycles under 4 C charging conditions—a substantial improvement over the 12 cycles observed for uncoated anodes (Fig. 4f). The remarkable enhancement in cyclability at high charging rates was attributed to the ability of artificial interphases to expedite charge transfer, eliminate the SEI formation, and reduce interphase impedance by over 75%. Additionally, a robust bifunctional Li_3P interphase, firmly affixed to the graphite surface, has been shown to facilitate rapid Li^+ de-solvation and accelerate Li^+ transport across the SEI, thereby achieving stable cyclability and enhanced fast-charging capabilities at low temperatures[14]. The dense, continuous, and robust nature of the Li_3P interphase is credited with enhancing charge transport kinetics and enabling swift Li^+ transfer across the SEI (Fig. 4g). Furthermore, the introduction of a Li^+ conductive and electron/solvent-repelling MoO_x–MoN_x interface on the graphite surface (Fig. 4h) has been identified as an effective strategy for bolstering fast-charging capabilities[38]. This interface supported rapid Li^+ diffusion while

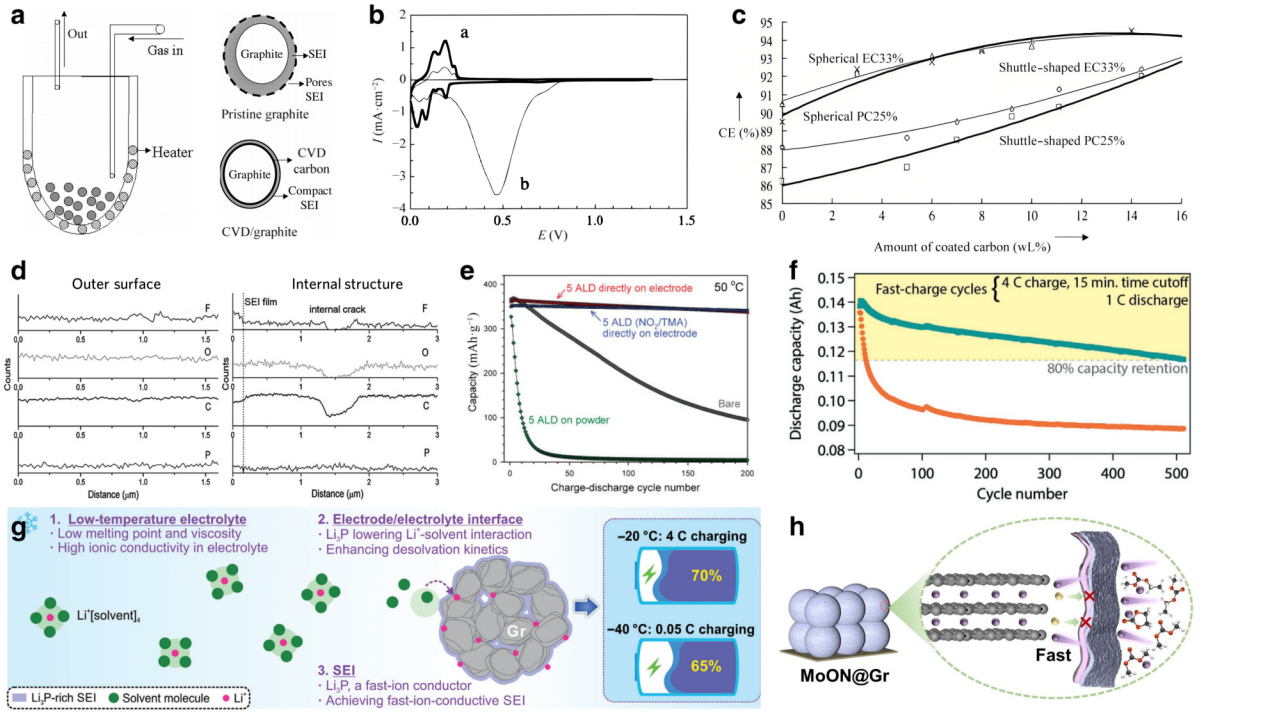

Fig. 4. Surface coating for the regulation of electrode interphase of graphite anodes. a, CVD-derived carbon coating layer promoting the formation of a compact and thin SEI. Reproduced with permission from Ref.[30], © Elsevier Science Ltd. 2001. **b**, TVD-derived coated graphite showing reduced electrolyte sensitivity. Reproduced with permission from Ref.[31], © The Electrochemical Society 2000. **c**, TVD-derived coated spherical natural graphite realizing high Coulombic efficiency in PC-based electrolytes. Reproduced with permission from Ref.[32], © WILEY-VCH Verlag GmbH & Co. KGaA, Weinheim 2023. **d**, Elemental line scan analysis indicating that the carbon coating layer inhibited the formation of internal SEI film in graphite anodes. Reproduced with permission from Ref.[33], © Elsevier Ltd. 2026. **e**, Ultrathin Al_2O_3 artificial interphase significantly improving the cyclability of graphite anodes at 50 °C. Reproduced with permission from Ref.[36], © WILEY-VCH Verlag GmbH & Co. KGaA, Weinheim 2010. **f**, Solid-state electrolyte coating of graphite anodes enabling fast-charging capability. Reproduced with permission from Ref.[37], © Wiley-VCH GmbH 2021. **g**, Schematic for Li_3P interphase on graphite simultaneously boosting the charge transport kinetics and fast Li^+ crossing the SEI. Reproduced with permission from Ref.[14], © Wiley-VCH GmbH 2023. **h**, Schematics showing MoO_x–MoN_x interface allowing fast Li^+ diffusion yet blocking solvent access and electron leakage. Reproduced with permission from Ref.[38], © Wiley-VCH GmbH 2024.

simultaneously preventing solvent access and electron leakage, resulting in a retention of 340.3 mAh·g^{-1} after 4000 cycles at 6 C. The aforementioned studies underscore the potential of Li^+ conductive interphase on graphite anodes among the most promising approaches for augmenting the fast-charging capability and broadening the operation temperature range of LIBs.

5 Electrolyte regulation

The SEI layer, which forms at the surface of graphite anodes during charging, is pivotal in stabilizing the anode–electrolyte interface[39]. It plays a crucial role in preventing further decomposition of electrolyte and facilitating efficient Li^+ ion transportation[40]. Given that the SEI arises from the reductive decomposition of the electrolyte, its composition and structure are intrinsically linked to the constituents of working electrolyte. Consequently, the optimization of electrolyte components—encompassing solvents, additives, and lithium salts—holds the potential to significantly influence the characteristics of SEI. By meticulously adjusting these components, it is possible to tailor the SEI to achieve desired properties, such as enhanced stability and fast Li^+ diffusion. Therefore, optimizing the formulation of electrolytes emerges as a critical approach in the design and performance enhancement of graphite anodes. More robust and efficient LIBs can be fabricated by leveraging a deeper understanding of the interplay between electrolyte composition and the derived-SEI.

Incorporating film-forming additives into the electrolyte is a pivotal strategy for augmenting the stability and performance of the SEI on graphite anodes. Ester additives, such as vinylene carbonate (VC), vinylidene ethylene carbonate (VEC), and fluoroethylene carbonate (FEC), along with sulfur-containing additives like propane sultone (PS), ethylene sulfite (ES), and 1,3,2-dioxathiolane-2,2-dioxide (DTD), possess a higher reduction potential than conventional solvents, such as EC. It enables these additives to decompose preferentially at the electrode surface, forming a protective film that significantly influences the composition, structure, and properties of SEI. VC and VEC, in particular, are known to form polymeric films during the initial SEI formation due to their elevated reduction potential[41]. When used judiciously, these additives are commonly integrated into Li-ion pouch cells to enhance the mechanical robustness and stability of the SEI, thereby minimizing irreversible capacity loss and gas evolution[18]. FEC is particularly adept at forming a robust and stable SEI enriched with lithium fluoride (LiF), which enhances ionic conductivity and encourages the densification of the SEI film[42, 43]. The incorporation of FEC has been shown to yield a stable and elastic SEI capable of withstanding substantial volume changes, therefore preserving the electrode interphase and improving the cyclability of Si-C anodes[44]. Sulfur-containing additives contribute to the formation of an SEI containing sulfur species and LiF, which is characterized by lower

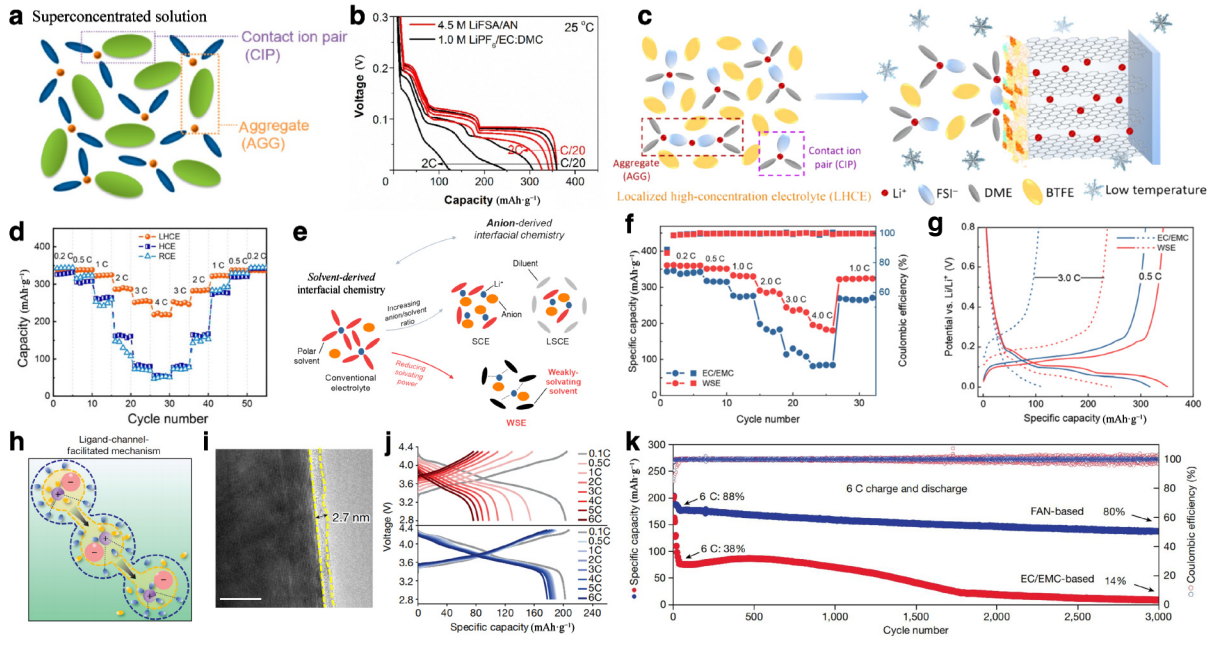

Fig. 5. Electrolyte optimization for the regulation of electrode interphase of graphite anodes. a, Schematic of the solvation structure of HCE (4.5 M LiFSI in acetonitrile), and **b**, graphite anodes in this electrolyte showing improved lithiation capability. Reproduced with permission from Ref. [51], © American Chemical Society 2014. **c**, Schematic of LHCE and its derived-SEI on the graphite anodes, and **d**, significantly improved fast-charge capability. Reproduced with permission from Ref.[53], © Wiley-VCH GmbH 2020. **e**–**g**, Schematic of of WSE (e), and improved rate performance (f) with corresponding voltage profiles (g) of graphite anodes. Reproduced with permission from Ref.[55], © Wiley-VCH GmbH 2020. **h**–**k**, Ligand-channel-facilitated mechanism in designed electrolyte using small-sized solvent with weak solvation energy (h), TEM image revealing the uniform and thin SEI on the graphite anodes (i), significantly improved charge capability (j), and cycling stability at high charge-rate of 6 C (k). Reproduced with permission from Ref.[56], © Lu, D. et al. 2024.

impedance, reduced charge transfer resistance, and elevated ionic conductivity. These attributes have rendered sulfur-containing additives a staple in low-temperature electrolytes[45]. The strategic use of film-forming additives is essential in optimizing the SEI on graphite anodes. By employing these additives with precision and acumen, it is feasible to modulate the composition and properties of SEI layers, culminating in substantial enhancements in the electrochemical performance of batteries[46].

Beyond the use of film-forming additives, the optimization of salts and solvents in the electrolyte is a critical approach to regulate the solvation structure of Li ions[47, 48], which in turn significantly influences the composition and structure of the resulting SEI[49]. By elevating the salt concentration to 3–5 M, highly concentrated electrolytes (HCEs) can be formulated[50]. These electrolytes enhance the interactions between solvated Li ions and anions, effectively reducing the presence of free solvent molecules (Fig. 5a)[51]. A key advantage of HCEs is their capability to form a salt-derived SEI on anode surfaces[49]. Reversible Li^+ intercalation/deintercalation with markedly faster kinetics compared to those in commercial electrolytes can be achieved (Fig. 5b), which is a breakthrough unattainable with the standard 1.0 M salt concentration[51]. Furthermore, a 5 V-class $LiNi_{0.5}Mn_{1.5}O_4$|graphite battery, when operated with a nonflammable HCE (5.3 M LiFSI in trimethyl phosphate), demonstrated stable cyclability and minimal capacity decay over 100 cycles at 0.2 C, along with a high Coulombic efficiency of 99.2%[52]. The enhanced performance of graphite anodes using HCEs is attributed to the robust, salt-derived inorganic SEI, which facilitates compatibility with functional solvents that are typically incompatible with graphite anodes in standard electrolytes at 1.0 M salt concentration.

To address the limitations of HCEs, such as reduced ionic conductivity and increased viscosity, localized high-concentration electrolytes (LHCEs) have been developed (Fig. 5c)[53]. They incorporate a low-polarity diluent solvent that minimally interacts with Li^+ ions. Utilizing an LHCE (1.5 M LiFSI in dimethoxyethane with bis(2,2,2-trifluoroethyl)ether as the diluent), graphite anodes exhibited fast-charging capability (220 mAh·g^{-1} at 4 C) (Fig. 5d) and stable cyclability (85.5% capacity retention after 200 cycles at 4 C), along with exceptional low-temperature performance. The improvement is primarily attributed to the LHCE-derived uniform and robust SEI, which facilitates rapid ion transfer and prevents co-intercalation of ether solvents.

Without the need of increased salt concentrations or costly fluorine diluents, the formation of a unique anion-derived SEI[54] on graphite electrodes can be realized using weakly solvating electrolytes (WSEs). These WSEs consist of pure non-polar solvents and maintain a low salt concentration of 1 M (Fig. 5e)[55]. Graphite anodes with a WSE (1.0 M LiFSI in 1,4-dioxane) as the electrolyte displayed fast-charging capability (Figs. 5f and 5g) and long-term cycling stability, which was attributed to the unique anion-derived SEI and its enhanced interfacial kinetics.

Recently, a novel electrolyte design concept has emerged, employing small-sized solvents with low solvation energy (Fig. 5h)[56]. This approach aims to create fast ion-conduction ligand channels to enhance Li^+ transport in electrolytes and enable the formation of an inorganic-rich SEI on graphite anodes (Fig. 5i). As a prototype, a 1.3 M LiFSI in fluoroacetonitrile electrolyte was proposed, showcasing ultrahigh ionic conductivity of 40.3 mS·cm^{-1} at 25 °C and an impressive 11.9 mS·cm^{-1} even at −70 °C. This potent electrolyte enables LIBs with graphite anodes to exhibit significantly improved fast-charging capability (Fig. 5j) and a high-capacity retention of 80% after 3000 cycles at 6 C (Fig. 5k).

Electrolyte optimization is a promising avenue for constructing a powerful electrode interphase on graphite anodes, thereby enhancing interfacial charge transfer kinetics[57, 58]. It enables to improved fast-charging capabilities[59] and low-temperature performance in LIBs[60]. A cost-effective electrolyte optimization strategy is essential for the practical application and commercial viability of these advanced energy storage technologies.

6 Anode interphase regulation

Anode materials characterized by high capacity and low delithiation potential are advantageous for enhancing the operating voltage and energy density of full cell systems. Integrating the benefits of lithium metal anodes (theoretical capacity of 3860 mAh·g^{-1} and −3.04 V vs. standard hydrogen electrode)[61–63] into graphite anodes can yield high-performance graphite/lithium composite anodes with high capacity and reduced lithium storage potential.

Although lithium plating on graphite anodes has been rigorously avoided due to the safety hazards associated with lithium dendrites that can cause short-circuiting[64–67], recent research indicates that reversible lithium plating/stripping on graphite anodes can be achieved through strategic interphase regulation[68]. Utilizing LHCE to form an anion-derived interphase on the graphite surface, a uniform lithium plating distribution can be achieved, thereby minimizing the presence of dead lithium[20]. This approach resulted in an average Coulombic efficiency of approximately 99.5% for the deposited lithium during reversible plating/stripping. Thanks to the controlled lithium plating (Fig. 6a) and superior Coulombic efficiency, a $LiNi_{0.5}Mn_{0.3}Co_{0.2}O_2$|graphite cell demonstrated impressive capacity retention of 80.2% over 500 cycles. Employing an LHCE (1.6 M LiFSI in DMC: EC: 1,1,2,2-tetrafluoroethyl-2,2,3,3-tetrafluor-opropyl ether with 30:1:40 by volume) to create a LiF-rich SEI on graphite anodes, an even higher average Coulombic efficiency of 99.9% over 240 cycles and a reversibility of 99.95% for lithium plating is attainable[69]. This is particularly noteworthy given that lithium plating contributed to 40% of the total lithiation capacity (Fig. 6b).

To prevent the accumulation of dead lithium, which restricts Li^+ transportation and continuously increases the overpotential of lithium stripping, a conversion-deintercalation (CTD) delithiation mechanism has been proposed (Fig. 6c)[70]. This mechanism manipulates the anode's overpotential to suppress the generation of dead lithium. Under practical conditions, a full cell employing the CTD delithiation mechanism sustained 210 cycles with an 80% capacity retention, outperforming a bare lithium anode lasting for only 110 cycles. This significant enhancement is primarily attributed to the activation of deintercalation reaction when the anode's overpotential exceeds that of lithiated graphite. This reaction completes the CTD delithiation process, significantly reducing the formation of dead lithium due to the highly reversible nature of the deintercalation reaction in graphite. Consequently, the regulation of the graphite anode interphase is pivotal for achieving reversible lithium plating/stripping with high Coulombic efficiency[71].

Graphite anodes are poised to play a pivotal role in the realm of next-generation energy storage technologies, including potassium-ion batteries[72–76], dual-ion batteries[77], and calcium-ion batteries[78, 79].

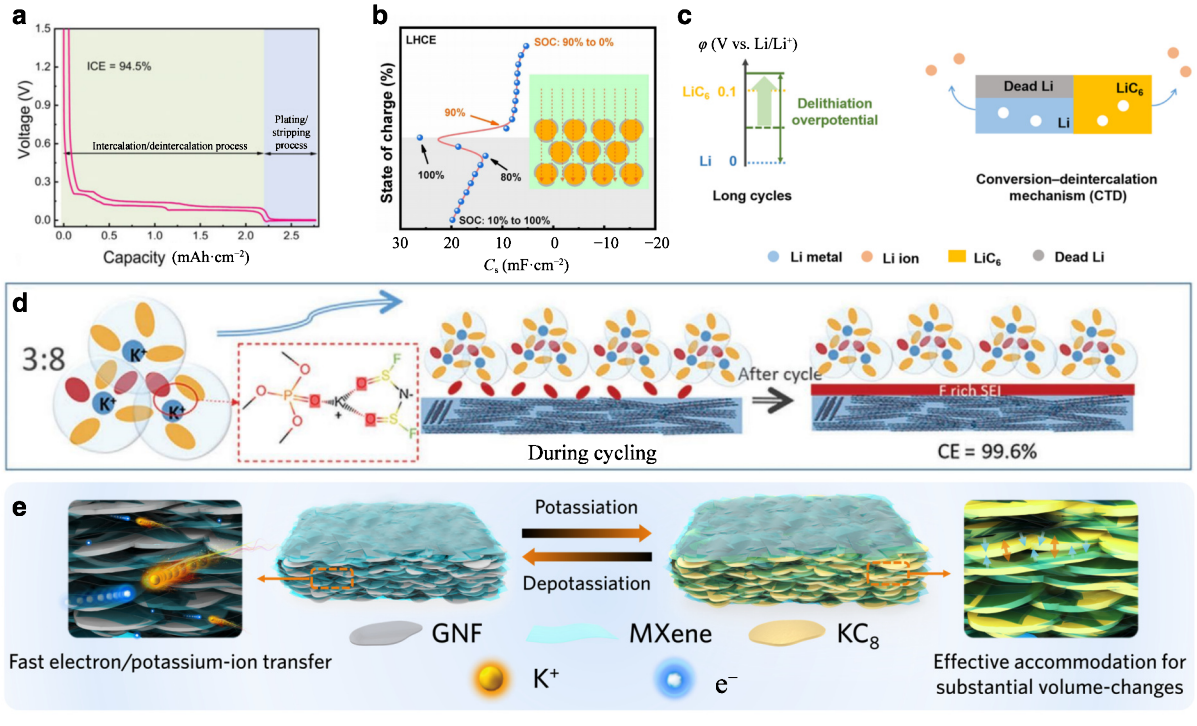

Fig. 6. Regulating anode interphase for emerging energy storage technologies. a, The robust inorganic SEI derived from LHCE on the graphite realizing reversible lithium plating/striping under the endurable amount of lithium. Reproduced with permission from Ref.[20], © Wiley-VCH GmbH 2021. **b**, Li plating-reversible graphite anode via using a LHCE successfully regulate the Li plating with high reversibility. Reproduced with permission from Ref.[69], © Wiley-VCH GmbH 2023. **c**, Conversion–deintercalation mechanism proposed by manipulating the overpotential of the anode to restrain the generation of dead Li. Reproduced with permission from Ref.[70], © American Chemical Society 2021. **d**, A F-rich interphase on graphite anodes during potassium storage is realized by using HCE. Reproduced with permission from Ref.[85], © Wiley-VCH GmbH 2020. **e**, $Ti_3C_2T_x$ nanosheets as a multi-functional electrode framework with electron/potassium-ion dual-conducting capability to ensure stable graphite interphase with stable cyclability. Reproduced with permission from Ref.[88], © Wiley-VCH GmbH 2021.

In these systems, the regulation of the graphite interphase is a critical factor for achieving optimal performance. For instance, the electrode interphase undergoes significant changes during potassium storage cycling due to an approximate 60% expansion in the interlayer distance of graphite anodes at full potassiation, and therefore its stability is paramount to the electrochemical performance[72, 74, 75, 80, 81]. Strategically optimizing the electrolyte with cyclic ethers[82], HCE (Fig. 6d)[83–85], LHCE[86], and WSE[87] can facilitate the formation of a stable anion-derived SEI on graphite anodes, thereby enhancing stable cyclability. Additionally, $Ti_3C_2T_x$ MXene nanosheets, known for their dual-function as fast electron and potassium-ion conductors, are integrated into the framework of all-integrated graphite nanoflake/MXene electrodes (GNFM)[88]. This integration leverages the unique properties of MXene, such as its 2D morphology, metallic conductivity[89, 90], and flexibility. The robust and flexible MXene framework ensures a stable electrode interphase and expedites electron/potassium-ion transfer, conferring GNFM electrodes with stable cyclability and superior rate performance (Fig. 6e). Furthermore, by modulating the anion species in nonaqueous electrolytes, the co-intercalation of solvated calcium ions in graphite can be realized, leading to higher reversible capacities, accelerated intercalation kinetics, and improved reversibility[79].

7 Current status of graphite anode industrialization

Anode materials, as an indispensable part of LIBs, play a decisive role in cycle life, fast-charging performance, temperature tolerance, energy density, and power density. With the advancement of technology, anode materials have evolved from natural graphite to diversified materials that includes natural graphite, artificial graphite, lithium titanate, soft carbon, hard carbon, silicon-carbon composites, and more. Natural graphite with lower cost and high lithium storage capacity is the preferred choice for achieving high energy density in LIBs, especially for consumer electronics. Artificial graphite, known for its excellent cycling stability and comprehensive performance, has secured a significant position in the market for power batteries. Although innovative anode materials such as lithium titanate and silicon-based anodes show great potential, they are still in the trial phase and have not yet reached the stage of large-scale commercial application.

Graphite anode materials, with their exceptional performance and a dominant market share of 97% in China since 2022, have become the preferred choice for commercialized LIBs. Graphite anodes can be divided into two categories: natural graphite and artificial graphite. Natural graphite, derived from highly crystalline flake graphite, undergoes a meticulous manufacturing process that includes crushing, grading, purification, spheroidization, and surface coating treatment. However, the high reactivity at the edge sites of natural graphite leads to poor compatibility with electrolytes and an unstable SEI, which cause the degradation of layered structure during lithium storage and correspondingly affect the cyclability[32]. Therefore, surface modification of natural graphite is a crucial step to enhance its performance. Artificial graphite, on the other hand, is meticulously prepared from materials that are easily graphitizable, such as pitch, coke, petroleum coke, and needle coke, through a series of processes including crushing, shaping, mixing, granulating, graphitization, sieving, and surface coating. Parameters of the graphitization treatment, particularly the temperature and duration of heat treatment, plays a vital role in the degree of graphitization of the prepared artificial graphite, thereby affecting its reversible lithium storage capacity. Moreover, the granulating and sieving steps determine the particle size distribution and specific surface area of the anode materials, which directly impact the ICE and rate performance. With its outstanding comprehensive performance, artificial graphite meets the stringent requirements for anodes of power LIBs. As the demand for power batteries in electric vehicles surges, the annual shipment of artificial graphite has seen a sharp increase since 2018 in China (Fig. 7a). After 2019, the market share of artificial graphite in the graphite anode sector has exceeded 80%, making it the mainstream anode material. It is projected that the market demand for artificial graphite anode materials will exceed 2 million tons by 2025.

Natural graphite faces challenges in the field of power batteries, particularly in cycling life and rate capability. In contrast, artificial graphite anodes, treated by graphitization, demonstrate superior structural stability and lower volume expansion, resulting in stable cyclability. Moreover, the high compatibility of artificial graphite with organic electrolytes, when paired with specialized functional electrolytes, achieves optimal low-temperature performance, rate capability, and fast-charging capabilities. As summarized in Table 1, the superior comprehensive performance indicators of artificial graphite make it a better choice for the fields of power and high-

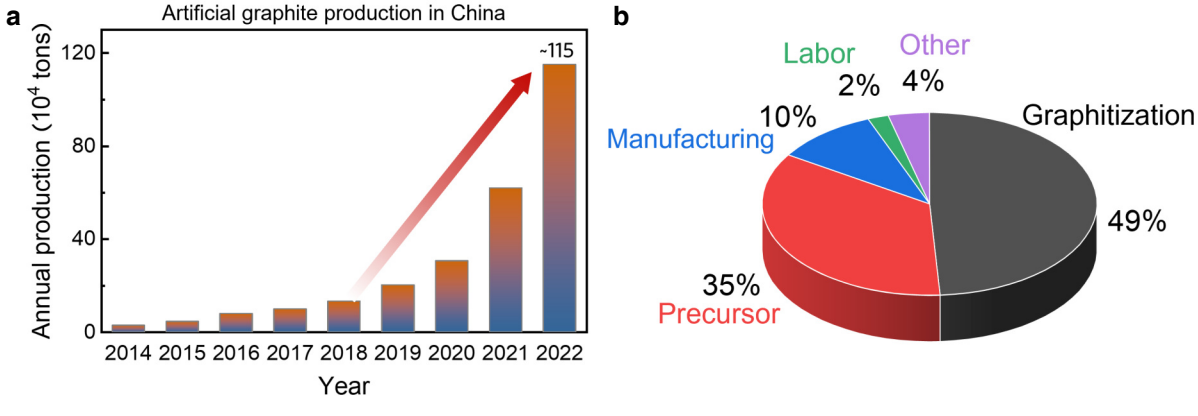

Fig. 7. Annual production and cost analysis of artificial graphite anodes in China. a, The annual production of artificial graphite in China market from 2014 to 2022. **b**, The cost analysis for producing artificial graphite anodes.

Table 1 Performance comparison between artificial graphite and natural graphite anodes.

	Artificial graphite	Natural graphite
Capacity	300–360 mAh·g^{-1}	340–370 mAh·g^{-1}
Initial Coulombic efficiency	90%–95%	91%–95%
Cyclability	High	Medium
Fast-charging performance	High	Medium
Electrolyte compatibility	High	Poor
Material density	High	Medium
Electrode volume expansion	Low	High
Cost	High	Low
Market share in graphite anode since 2020	~ 85%	~ 15%

end consumer batteries, with its market penetration rate gradually increasing. However, compared to natural graphite anodes, the main disadvantage of artificial graphite is its relatively higher cost. The cost of graphitization treatment and graphitizable precursors account for 49% and 35% of the manufacturing cost of artificial graphite anodes (Fig. 7b), respectively. Therefore, optimizing raw material selection and decreasing the cost of graphitization processing are effective ways to further enhance the competitiveness of artificial graphite anodes. Currently, many graphite anode manufacturers are committed to technological improvements and process innovations to enhance the utilization rate of raw materials and production efficiency, while exploring new technologies to reduce energy consumption and production costs in the graphitization process. With the retirement of a large number of power batteries, adopting environmental friendly and efficient new regenerative technologies to recover materials from spent LIBs can not only reduce environmental pollution but also promote the sustainable development of LIBs industry[91–94]. Efficient recycling of graphite anodes[95–97] from spent LIBs may help to reduce the production costs of artificial graphite, thereby obtaining cost-effective anode materials. The realization of this goal depends on the development of advanced recycling technologies[98–101]. For natural graphite anodes with advantage of inherent cost-effectiveness, the integration of advanced surface modification technologies to establish a stable electrode interface is essential to achieving superior electrochemical performance. Such advancements are pivotal in fulfilling the stringent requirements of high-power LIBs, potentially broadening their applications, and bolstering market penetration.

8 Outlook and conclusions

Graphite materials have been used as the anode of LIBs for almost 30 years. The development and application of graphite anodes still hold broad prospects. Looking ahead, we propose the following insights for carbon anodes:

(1) Graphite has achieved significant success in the field of LIBs. With the rise of new energy sources and the electrification of transportation and industry, the demand for graphite anodes continues to grow. The natural graphite requires effective spheroidization and surface modification to overcome the anisotropy in kinetics, anisotropic volume expansion, and unstable interphase. Artificial graphite made from different raw materials varies in properties and should be carefully selected based on user needs. Hard carbon shows great potential in the Na-ion batteries field and does not require a high-temperature graphitization treatment. The carbon-silicon composite anodes prepared from silanes[102–104] is strongly considered for high energy density batteries, in which the nanosized silicon can exhibit stable cyclability with a very long lifetime. The optimization of carbon-lithium metal composite anode[105–107] is also strongly considered, especially for solid state batteries.

(2) The production of artificial graphite anodes necessitates undergoing two critical thermal processes: carbonization and graphitization, with the latter requiring temperatures above 2800 °C. Graphitization treatment is both costly and highly energy-intensive process. Therefore, reducing carbon emissions and energy consumption in the artificial graphite manufacturing by innovative graphitization technologies is strongly considered.

(3) As the battery industry becomes more specialized, establishing data associations and data-driven models[108] to collect performance characteristics of LIBs in practical conditions is crucial to predict the battery life, in-depth understanding of the characteristics of graphite electrodes in various dynamic processes, and optimizing the factors for preparing LIBs cells, such as adjusting electrode preparation and usage of electrolyte, which is an important way to improve performance of LIBs.

(4) Lithium plating in graphite electrodes is a technical challenge, affecting the safety performance critically. It is urgent to monitoring the formation of lithium dendrite and mitigate its side-impacts. With the development of silicon-carbon anodes and composite lithium anodes, these fundamental principles will also guide the application of these new types of electrodes for high-energy-density LIBs.

(5) Interface regulation is key to promoting the high-quality development of graphite. This requires a combination of basic theoretical research, *in-situ* or *operando* characterization techniques, and data-driven process development.

(6) The recycling of electrode materials, especially graphite, from spent batteries is a developing industry direction. It is necessary to consider comprehensively the energy consumption, emissions, costs, and material properties in the recycling process.

Graphite-based anode materials not only have a wide range of applications in LIBs but also show application prospects in emerging energy storage technologies, such as potassium-ion batteries, dual-ion batteries, and calcium-ion batteries. Carbon materials have joined our life for thousands of years. This is an era full of opportunities because the demand and requirements of high-performance carbon materials are higher than ever; at the same time, it is also an era full of challenges as our understanding of the interface of carbon materials is still limited, and precise synthesis technology still has a long way to go. The current era urgently needs efficient preparation technologies with low or even negative carbon

emissions to produce better carbon materials for building a better life.

The interphase regulation engineering for graphite anodes is essential for the development of a robust and high-performing electrode interphase. The structure and composition of the SEI on graphite anodes are paramount, as they dictate the stability of the interphase, compatibility with electrolytes, and the kinetics of interfacial charge transfer. These factors collectively influence the long-term cyclability, fast-charging capability, temperature tolerance, and safety performance of LIBs. Despite longstanding role of graphite as the anode material in LIBs for nearly three decades, the investigation into the interphasial chemistry of graphite anodes continues to evolve. The seemingly minute SEI on graphite anodes can have a profound impact on the overall performance of LIBs. Advancing research in the area of interphase regulation, employing cost-effective, scalable, and advanced technologies, is crucial for the evolution of more powerful LIBs. Such advancements are instrumental in reducing carbon emissions, alleviating energy crises, and fostering the sustainable development of modern society.

References

[1] Mizushima, K.; Jones, P. C.; Wiseman, P. J.; Goodenough, J. B. Li_xCoO_2 ($0<x\leq1$): A new cathode material for batteries of high energy density. *Mater. Res. Bull.* **1980**, *15*, 783–789.

[2] Thackeray, M. M.; Johnson, P. J.; De Picciotto, L. A.; Bruce, P. G.; Goodenough, J. B. Electrochemical extraction of lithium from $LiMn_2O_4$. *Mater. Res. Bull.* **1984**, *19*, 179–187.

[3] Yoshino, A. From polyacetylene to carbonaceous anodes. *Nat. Energy* **2021**, *6*, 449.

[4] Zhang, H.; Yang, Y.; Ren, D. S.; Wang, L.; He, X. M. Graphite as anode materials: Fundamental mechanism, recent progress and advances. *Energy Storage Mater.* **2021**, *36*, 147–170.

[5] Yazami, R.; Touzain, P. A reversible graphite-lithium negative electrode for electrochemical generators. *J. Power Sources* **1983**, *9*, 365–371.

[6] Fong, R.; Von Sacken, U.; Dahn, J. R. Studies of lithium intercalation into carbons using nonaqueous electrochemical cells. *J. Electrochem. Soc.* **1990**, *137*, 2009–2013.

[7] Xu, K. Li-ion battery electrolytes. *Nat. Energy* **2021**, *6*, 763.

[8] Yan, C.; Xu, R.; Xiao, Y.; Ding, J. F.; Xu, L.; Li, B. Q.; Huang, J. Q. Toward critical electrode/electrolyte interfaces in rechargeable batteries. *Adv. Funct. Mater.* **2020**, *30*, 1909887.

[9] Zhu, K. M.; Kramer, D.; Peng, C. Edge and lithium concentration effects on intercalation kinetics for graphite anodes. *J. Energy Chem.* **2024**, *90*, 337–347.

[10] Yan, C.; Yao, Y. X.; Cai, W. L.; Xu, L.; Kaskel, S.; Park, H. S.; Huang, J. Q. The influence of formation temperature on the solid electrolyte interphase of graphite in lithium ion batteries. *J. Energy Chem.* **2020**, *49*, 335–338.

[11] Flandrois, S.; Simon, B. Carbon materials for lithium-ion rechargeable batteries. *Carbon* **1999**, *37*, 165–180.

[12] Yoshio, M.; Brodd, R. J.; Kozawa, A. *Lithium-Ion Batteries: Science and Technologies*; Springer: New York, 2009.

[13] Sawai, K.; Ohzuku, T. Factors affecting rate capability of graphite electrodes for lithium-ion batteries. *J. Electrochem. Soc.* **2003**, *150*, A674–A678.

[14] Huang, Y. S.; Wang, C. N.; Lv, H. F.; Xie, Y. S.; Zhou, S. Y.; Ye, Y. D.; Zhou, E.; Zhu, T. Y.; Xie, H. Y.; Jiang, W. et al. Bifunctional interphase promotes Li^+ de-solvation and transportation enabling fast-charging graphite anode at low temperature. *Adv. Mater.* **2024**, *36*, 2308675.

[15] Yu, L. G.; Yao, N.; Gao, Y. C.; Fu, Z. H.; Jiang, B.; Li, R. P.; Tang, C.; Chen, X. Probing the electric double layer structure at nitrogen-doped graphite electrodes by constant-potential molecular dynamics simulations. *J. Energy Chem.* **2024**, *93*, 299–305.

[16] Yao, Y. X.; Yao, N.; Zhou, X. R.; Li, Z. H.; Yue, X. Y.; Yan, C.; Zhang, Q. Ethylene-carbonate-free electrolytes for rechargeable Li-ion pouch cells at sub-freezing temperatures. *Adv. Mater.* **2022**, *34*, 2206448.

[17] Parimalam, B. S.; MacIntosh, A. D.; Kadam, R.; Lucht, B. L. Decomposition reactions of anode solid electrolyte interphase (SEI) components with $LiPF_6$. *J. Phys. Chem. C* **2017**, *121*, 22733–22738.

[18] Ota, H.; Sakata, Y.; Inoue, A.; Yamaguchi, S. Analysis of vinylene carbonate derived SEI layers on graphite anode. *J. Electrochem. Soc.* **2004**, *151*, A1659.

[19] Yao, Y. X.; Chen, X.; Yao, N.; Gao, J. H.; Xu, G.; Ding, J. F.; Song, C. L.; Cai, W. L.; Yan, C.; Zhang, Q. Unlocking charge transfer limitations for extreme fast charging of Li-ion batteries. *Angew. Chem., Int. Ed.* **2023**, *62*, e202214828.

[20] Cai, W. L.; Yan, C.; Yao, Y. X.; Xu, L.; Chen, X. R.; Huang, J. Q.; Zhang, Q. The boundary of lithium plating in graphite electrode for safe lithium-ion batteries. *Angew. Chem., Int. Ed.* **2021**, *60*, 13007–13012.

[21] Ren, X. C.; Zhang, X. Q.; Xu, R.; Huang, J. Q.; Zhang, Q. Analyzing energy materials by cryogenic electron microscopy. *Adv. Mater.* **2020**, *32*, 1908293.

[22] Yousaf, M.; Naseer, U.; Imran, A.; Li, Y. J.; Aftab, W.; Mahmood, A.; Mahmood, N.; Zhang, X.; Gao, P.; Lu, Y. Y. et al. Visualization of battery materials and their interfaces/interphases using cryogenic electron microscopy. *Mater. Today* **2022**, *58*, 238–274.

[23] Han, B.; Zou, Y. C.; Xu, G. Y.; Hu, S. G.; Kang, Y. Y.; Qian, Y. X.; Wu, J.; Ma, X. M.; Yao, J. Q.; Li, T. T. et al. Additive stabilization of SEI on graphite observed using cryo-electron microscopy. *Energy Environ. Sci.* **2021**, *14*, 4882–4889.

[24] Xu, L.; Xiao, Y.; Yu, Z. X.; Yang, Y.; Yan, C.; Huang, J. Q. Revisiting the electrochemical impedance spectroscopy of porous electrodes in Li-ion batteries by employing reference electrode. *Angew. Chem., Int. Ed.*, in press, DOI: 10.1002/anie.202406054.

[25] Steinhauer, M.; Risse, S.; Wagner, N.; Friedrich, K. A. Investigation of the solid electrolyte interphase formation at graphite anodes in Lithium-ion batteries with electrochemical impedance spectroscopy. *Electrochim. Acta* **2017**, *228*, 652–658.

[26] Xu, L.; Xiao, Y.; Yang, Y.; Yang, S. J.; Chen, X. R.; Xu, R.; Yao, Y. X.; Cai, W. L.; Yan, C.; Huang, J. Q. et al. *Operando* Quantified lithium plating determination enabled by dynamic capacitance measurement in working Li-ion batteries. *Angew. Chem., Int. Ed.* **2022**, *61*, e202210365.

[27] Lu, Y.; Zhao, C. Z.; Huang, J. Q.; Zhang, Q. The timescale identification decoupling complicated kinetic processes in lithium batteries. *Joule* **2022**, *6*, 1172–1198.

[28] Yan, W. G.; Chen, Z. T.; Ma, S. Y.; Chen, S.; Lu, Y.; Wang, M.; Chen, L.; Huang, Q.; Wang, B.; Su, Y. et al. Unraveling the relationship between the mineralogical characteristics and lithium storage performance of natural graphite anode materials. *Carbon* **2024**, *227*, 119270.

[29] Kuribayashi, I.; Yokoyama, M.; Yamashita, M. Battery characteristics with various carbonaceous materials. *J. Power Sources* **1995**, *54*, 1–5.

[30] Natarajan, C.; Fujimoto, H.; Tokumitsu, K.; Mabuchi, A.; Kasuh, T. Reduction of the irreversible capacity of a graphite anode by the CVD process. *Carbon* **2001**, *39*, 1409–1413.

[31] Yoshio, M.; Wang, H. Y.; Fukuda, K.; Hara, Y.; Adachi, Y. Effect of carbon coating on electrochemical performance of treated natural graphite as lithium-ion battery anode material. *J. Electrochem. Soc.* **2000**, *147*, 1245–1250.

[32] Yoshio, M.; Wang, H. Y.; Fukuda, K. Spherical carbon-coated natural graphite as a lithium-ion battery-anode material. *Angew. Chem., Int. Ed.* **2003**, *42*, 4203–4206.

[33] Zhang, H. L.; Liu, S. H.; Li, F.; Bai, S.; Liu, C.; Tan, J.; Cheng, H. M. Electrochemical performance of pyrolytic carbon-coated natural graphite spheres. *Carbon* **2006**, *44*, 2212–2218.

[34] Cai, W. L.; Yan, C.; Yao, Y. X.; Xu, L.; Xu, R.; Jiang, L. L.; Huang, J. Q.; Zhang, Q. Rapid lithium diffusion in order@disorder pathways for fast-charging graphite anodes. *Small Struct.* **2020**, *1*, 2000010.

[35] Zheng, B.; Zhou, W.; Liu, H.; Chen, S.; Gao, P.; Wang, Z. Y.; Liu, J. L. Surface chemistry induced robust SEI on graphite surface via soft carbon coating enables fast lithium storage. *Carbon* **2024**, *218*, 118729.

[36] Jung, Y. S.; Cavanagh, A. S.; Riley, L. A.; Kang, S. H.; Dillon, A. C.; Groner, M. D.; George, S. M.; Lee, S. H. Ultrathin direct atomic layer deposition on composite electrodes for highly durable and safe Li-ion batteries. *Adv. Mater.* **2010**, *22*, 2172–2176.

[37] Kazyak, E.; Chen, K. H.; Chen, Y. X.; Cho, T. H.; Dasgupta, N. P. Enabling 4C fast charging of lithium-ion batteries by coating graphite with a solid-state electrolyte. *Adv. Energy Mater.* **2022**, *12*, 2102618.

[38] Niu, M.; Dong, L. W.; Yue, J. P.; Li, Y. Q.; Dong, Y. Y.; Cheng, S. C.; Lv, S.; Zhu, Y. H.; Lei, Z. T.; Liang, J. Y. et al. A fast-charge graphite anode with a Li-ion-conductive, electron/solvent-repelling interface. *Angew. Chem., Int. Ed.* **2024**, *63*, e202318663.

[39] Sun, S. Y.; Zhang, X. Q.; Wang, Y. N.; Li, J. L.; Zheng, Z.; Huang, J. Q. Understanding the transport mechanism of lithium ions in solid-electrolyte interphase in lithium metal batteries with liquid electrolytes. *Mater. Today* **2024**, *77*, 39–65.

[40] Xie, Q. M.; Chen, J. W.; Xing, L. D.; Zhou, X. G.; Ma, Z. K.; Wu, B. H.; Lin, Y. L.; Zhou, H. B.; Li, W. S. Revealing the critical effect of solid electrolyte interphase on the deposition and detriment of Co(Ⅱ) ions to graphite anode. *J. Energy Chem.* **2022**, *69*, 389–396.

[41] Bhatt, M. D.; O'Dwyer, C. The role of carbonate and sulfite additives in propylene carbonate-based electrolytes on the formation of SEI layers at graphitic Li-ion battery anodes. *J. Electrochem. Soc.* **2014**, *161*, A1415–A1421.

[42] Yang, Z.; Zhou, X. Z.; Hao, Z. Q.; Chen, J.; Li, L.; Zhao, Q.; Lai, W. H.; Chou, S. L. Insight into the role of fluoroethylene carbonate on the stability of Sb||Graphite dual-ion batteries in propylene carbonate-based electrolyte. *Angew. Chem., Int. Ed.* **2024**, *63*, e202313142.

[43] Mei, W. X.; Jiang, L. H.; Zhou, H. M.; Sun, J. H.; Wang, Q. S. Correlating electrochemical performance and heat generation of Li plating for lithium-ion battery with fluoroethylene carbonate additive. *J. Energy Chem.* **2022**, *74*, 446–453.

[44] Wetjen, M.; Pritzl, D.; Jung, R.; Solchenbach, S.; Ghadimi, R.; Gasteiger, H. A. Differentiating the degradation phenomena in silicon-graphite electrodes for lithium-ion batteries. *J. Electrochem. Soc.* **2017**, *164*, A2840–A2852.

[45] Zhang, C. H.; Huo, S. D.; Su, B.; Bi, C. J.; Zhang, C.; Xue, W. D. Challenges of film-forming additives in low-temperature lithium-ion batteries: A review. *J. Power Sources* **2024**, *606*, 234559.

[46] Xia, Z. Y.; Zhou, K.; Lin, X. Y.; Xie, Z. Y. T.; Chen, Q. R.; Li, X. Q.; Cai, J.; Li, S. L.; Wang, H.; Xu, M. Q. et al. Rationally designing electrolyte additives for highly improving cyclability of $LiNi_{0.5}Mn_{1.5}O_4$/Graphite cells. *J. Energy Chem.* **2024**, *91*, 266–275.

[47] Cheng, H. R.; Sun, Q. J.; Li, L. L.; Zou, Y. G.; Wang, Y. Q.; Cai, T.; Zhao, F.; Liu, G.; Ma, Z.; Wahyudi, W. et al. Emerging era of electrolyte solvation structure and interfacial model in batteries. *ACS Energy Lett.* **2022**, *7*, 490–513.

[48] Li, Z. H.; Yao, Y. X.; Zheng, M. T.; Sun, S.; Yang, Y.; Xiao, Y.; Xu, L.; Jin, C. B.; Yue, X. Y.; Song, T. L. et al. Electrolyte design enables rechargeable $LiFePO_4$/Graphite batteries from −80°C to 80°C. *Angew. Chem., Int. Ed.*, in press, DOI: 10.1002/anie.202409409.

[49] Yao, Y. Y.; Yan, C.; Zhang, Q. Emerging interfacial chemistry of graphite anodes in lithium-ion batteries. *Chem. Commun.* **2020**, *56*, 14570–14584.

[50] Yamada, Y.; Wang, J. H.; Ko, S.; Watanabe, E.; Yamada, A. Advances and issues in developing salt-concentrated battery electrolytes. *Nat. Energy* **2019**, *4*, 269–280.

[51] Yamada, Y.; Furukawa, K.; Sodeyama, K.; Kikuchi, K.; Yaegashi, M.; Tateyama, Y.; Yamada, A. Unusual stability of acetonitrile-based superconcentrated electrolytes for fast-charging lithium-ion batteries. *J. Am. Chem. Soc.* **2014**, *136*, 5039–5046.

[52] Wang, J. H.; Yamada, Y.; Sodeyama, K.; Watanabe, E.; Takada, K.; Tateyama, Y.; Yamada, A. Fire-extinguishing organic electrolytes for safe batteries. *Nat. Energy* **2018**, *3*, 22–29.

[53] Jiang, L. L.; Yan, C.; Yao, Y. X.; Cai, W. L.; Huang, J. Q.; Zhang, Q. Inhibiting solvent co-intercalation in a graphite anode by a localized high-concentration electrolyte in fast-charging batteries. *Angew. Chem., Int. Ed.* **2021**, *60*, 3402–3406.

[54] Yan, C.; Jiang, L. L.; Yao, Y. X.; Lu, Y.; Huang, J. Q.; Zhang, Q. Nucleation and growth mechanism of anion-derived solid electrolyte interphase in rechargeable batteries. *Angew. Chem., Int. Ed.* **2021**, *60*, 8521–8525.

[55] Yao, Y. X.; Chen, X.; Yan, C.; Zhang, X. Q.; Cai, W. L.; Huang, J. Q.; Zhang, Q. Regulating interfacial chemistry in lithium-ion batteries by a weakly solvating electrolyte. *Angew. Chem., Int. Ed.* **2021**, *60*, 4090–4097.

[56] Lu, D.; Li, R. H.; Rahman, M. M.; Yu, P. Y.; Lv, L.; Yang, S.; Huang, Y. Q.; Sun, C. C.; Zhang, S. Q.; Zhang, H. K. et al. Ligand-channel-enabled ultrafast Li-ion conduction. *Nature* **2024**, *627*, 101–107.

[57] Tao, L.; Xia, D. W.; Sittisomwong, P.; Zhang, H. R.; Lai, J. W.; Hwang, S.; Li, T. Y.; Ma, B. Y.; Hu, A. Y.; Min, J. et al. Solvent-mediated, reversible ternary graphite intercalation compounds for extreme-condition Li-ion batteries. *J. Am. Chem. Soc.* **2024**, *146*, 16764–16774.

[58] Yang, Y. S.; Chen, Y. F.; Tan, L. L.; Zhang, J. W.; Li, N.; Ji, X.; Zhu, Y. J. Rechargeable $LiNi_{0.65}Co_{0.15}Mn_{0.2}O_2$||Graphite batteries operating at −60 °C. *Angew. Chem., Int. Ed.* **2022**, *61*, e202209619.

[59] Cai, W. L.; Yao, Y. X.; Zhu, G. L.; Yan, C.; Jiang, L. L.; He, C. X.; Huang, J. Q.; Zhang, Q. A review on energy chemistry of fast-charging anodes. *Chem. Soc. Rev.* **2020**, *49*, 3806–3833.

[60] Li, Z. H.; Yao, N.; Yu, L. G.; Yao, Y. X.; Jin, C. B.; Yang, Y.; Xiao, Y.; Yue, X. Y.; Cai, W. L.; Xu, L. et al. Inhibiting gas generation to achieve ultralong-lifespan lithium-ion batteries at low temperatures. *Matter* **2023**, *6*, 2274–2292.

[61] Liu, H.; Cheng, X. B.; Yan, C.; Li, Z. H.; Zhao, C. Z.; Xiang, R.; Yuan, H.; Huang, J. Q.; Kuzmina, E.; Karaseva, E. et al. A perspective on energy chemistry of low-temperature lithium metal batteries. *iEnergy* **2022**, *1*, 72–81.

[62] Yang, S. J.; Hu, J. K.; Jiang, F. N.; Yuan, H.; Park, H. S.; Huang, J. Q. Safer solid-state lithium metal batteries: Mechanisms and strategies. *InfoMat* **2024**, *6*, e12512.

[63] Xu, P.; Shuang, Z. Y.; Zhao, C. Z.; Li, X.; Fan, L. Z.; Chen, A. B.; Chen, H. T.; Kuzmina, E.; Karaseva, E.; Kolosnitsyn, V. et al. A review of solid-state lithium metal batteries through *in-situ* solidification. *Sci. China Chem.* **2024**, *67*, 67–86.

[64] Yang, Y.; Xu, L.; Yang, S. J.; Yan, C.; Huang, J. Q. Electrolyte inhomogeneity induced lithium plating in fast charging lithium-ion batteries. *J. Energy Chem.* **2022**, *73*, 394–399.

[65] Xu, Y. J.; Wang, B.; Wan, Y.; Sun, Y.; Wang, W. L.; Sun, K.; Yang, L. J.; Hu, H.; Wu, M. B. Understanding the process of lithium deposition on a graphite anode for better lithium-ion batteries. *New Carbon Mater.* **2023**, *38*, 678–693.

[66] Yang, Y.; Zhong, X. L.; Xu, L.; Yang, Z. L.; Yan, C.; Huang, J. Q. The principle and amelioration of lithium plating in fast-charging lithium-ion batteries. *J. Energy Chem.* **2024**, *97*, 453–459.

[67] Liu, S. Y.; Gu, B. Q.; Chen, Z. H.; Zhan, R. M.; Wang, X. C.; Feng, R. K.; Sun, Y. M. Suppressing dendritic metallic Li formation on graphite anode under battery fast charging. *J. Energy Chem.* **2024**, *91*, 484–500.

[68] Yan, S. S.; Chen, X. X.; Zhou, P.; Wang, P. C.; Zhou, H. Y.; Zhang,

W. L.; Xia, Y. C.; Liu, K. Regulating the growth of lithium dendrite by coating an ultra-thin layer of gold on separator for improving the fast-charging ability of graphite anode. *J. Energy Chem.* **2022**, *67*, 467–473.

[69] Yue, X. Y.; Zhang, J.; Dong, Y. T.; Chen, Y. M.; Shi, Z. Q.; Xu, X. J.; Li, X. L.; Liang, Z. Reversible Li plating on graphite anodes through electrolyte engineering for fast-charging batteries. *Angew. Chem. Int. Ed.* **2023**, *62*, e202302285.

[70] Shi, P.; Hou, L. P.; Jin, C. B.; Xiao, Y.; Yao, Y. X.; Xie, J.; Li, B. Q.; Zhang, X. Q.; Zhang, Q. A successive conversion-deintercalation delithiation mechanism for practical composite lithium anodes. *J. Am. Chem. Soc.* **2022**, *144*, 212–218.

[71] Xu, X. J.; Yue, X. Y.; Chen, Y. M.; Liang, Z. Li plating regulation on fast-charging graphite anodes by a triglyme-$LiNO_3$ synergistic electrolyte additive. *Angew. Chem., Int. Ed.* **2023**, *62*, e202306963.

[72] Jian, Z. L.; Luo, W.; Ji, X. L. Carbon electrodes for K-ion batteries. *J. Am. Chem. Soc.* **2015**, *137*, 11566–11569.

[73] Chang, X. Q.; Sun, N.; Zhou, H. Y.; Soomro, R. A.; Xu, B. Soft carbon-coated bulk graphite for improved potassium ion storage. *Chin. Chem. Lett.* **2023**, *34*, 107312.

[74] Cao, B.; Zhang, Q.; Liu, H.; Xu, B.; Zhang, S. L.; Zhou, T. F.; Mao, J. F.; Pang, W. K.; Guo, Z. P.; Li, A. et al. Graphitic carbon nanocage as a stable and high power anode for potassium-ion batteries. *Adv. Energy Mater.* **2018**, *8*, 1801149.

[75] Liu, H.; Du, H. L.; Zhao, W.; Qiang, X. J.; Zheng, B.; Li, Y.; Cao, B. Fast potassium migration in mesoporous carbon with ultrathin framework boosting superior rate performance for high-power potassium storage. *Energy Storage Mater.* **2021**, *40*, 490–498.

[76] Wang, D. K.; Zhang, J. P.; Dong, Y.; Cao, B.; Li, A.; Chen, X. H.; Yang, R.; Song, H. H. Progress on graphitic carbon materials for potassium-based energy storage. *New Carbon Mater.* **2021**, *36*, 435–448.

[77] Li, B.; Cao, B. B.; Zhou, X. X.; Zhang, Z. Z.; Dai, D. M.; Jia, M. M.; Liu, D. H. Pre-constructed SEI on graphite-based interface enables long cycle stability for dual ion sodium batteries. *Chin. Chem. Lett.* **2023**, *34*, 107832.

[78] Park, J.; Xu, Z. L.; Yoon, G.; Park, S. K.; Wang, J.; Hyun, H.; Park, H.; Lim, J.; Ko, Y. J.; Yun, Y. S. et al. Stable and high-power calcium-ion batteries enabled by calcium intercalation into graphite. *Adv. Mater.* **2020**, *32*, 1904411.

[79] Yi, Y. Y.; Xing, Y. D.; Wang, H.; Zeng, Z. H.; Sun, Z. T.; Li, R. J.; Lin, H. J.; Ma, Y. Y.; Pu, X. J.; Li, M. M. J. et al. Deciphering anion-modulated solvation structure for calcium intercalation into graphite for Ca-ion batteries. *Angew. Chem., Int. Ed.* **2024**, *63*, e202317177.

[80] Xiao, N.; Guo, H. D.; Xiao, J.; Wei, Y. B.; Ma, X. Q.; Zhang, X. Y.; Qiu, J. S. KOH-treated mesocarbon microbeads used as high-rate anode materials for potassium-ion batteries. *New Carbon Mater.* **2023**, *38*, 327–334.

[81] Wang, H. Y.; Du, H. W.; Zhang, H. C.; Meng, S. J.; Lu, Z. S.; Jiang, H.; Li, C. Z.; Wang, J. J. Regulated adsorption-diffusion and enhanced charge transfer in expanded graphite cohered with N, B bridge-doping carbon patches to boost K-ion storage. *J. Energy Chem.* **2023**, *76*, 67–74.

[82] Zhang, J. S.; Wu, J. F.; Wang, Z. X.; Mo, Y.; Zhou, W.; Peng, Y. F.; He, B. C.; Xiao, K. K.; Chen, S.; Xu, C. H. et al. Stabilizing SEI by cyclic ethers toward enhanced K^+ storage in graphite. *J. Energy Chem.* **2022**, *71*, 344–350.

[83] Fan, L.; Ma, R. F.; Zhang, Q. F.; Jia, X. X.; Lu, B. G. Graphite anode for a potassium-ion battery with unprecedented performance. *Angew. Chem., Int. Ed.* **2019**, *58*, 10500–10505.

[84] Liu, S. L.; Mao, J. F.; Zhang, Q.; Wang, Z. J.; Pang, W. K.; Zhang, L.; Du, A. J.; Sencadas, V.; Zhang, W. C.; Guo, Z. P. An intrinsically non-flammable electrolyte for high-performance potassium batteries. *Angew. Chem.* **2020**, *132*, 3667–3673.

[85] Liu, S. L.; Mao, J. F.; Zhang, L.; Pang, W. K.; Du, A. J.; Guo, Z. P. Manipulating the solvation structure of nonflammable electrolyte and interface to enable unprecedented stability of graphite anodes beyond 2 years for safe potassium-ion batteries. *Adv. Mater.* **2021**, *33*, 2006313.

[86] Qin, L.; Xiao, N.; Zheng, J. F.; Lei, Y.; Zhai, D. Y.; Wu, Y. Y. Localized high-concentration electrolytes boost potassium storage in high-loading graphite. *Adv. Energy Mater.* **2019**, *9*, 1902618.

[87] Li, J. F.; Hu, Y. Y.; Xie, H. B.; Peng, J.; Fan, L.; Zhou, J.; Lu, B. G. Weak cation-solvent interactions in ether-based electrolytes stabilizing potassium-ion batteries. *Angew. Chem., Int. Ed.* **2022**, *61*, e202208291.

[88] Cao, B.; Liu, H.; Zhang, P.; Sun, N.; Zheng, B.; Li, Y.; Du, H. L.; Xu, B. Flexible MXene framework as a fast electron/potassium-ion dual-function conductor boosting stable potassium storage in graphite electrodes. *Adv. Funct. Mater.* **2021**, *31*, 2102126.

[89] Liu, H.; Xu, Z. J.; Cao, B.; Xin, Z. J.; Lai, H. J.; Gao, S.; Xu, B.; Yang, J. L.; Xiao, T.; Zhang, B. et al. Marangoni-driven self-assembly MXene as functional membrane enables dendrite-free and flexible zinc-iodine pouch cells. *Adv. Energy Mater.* **2024**, *14*, 2400318.

[90] Cao, B.; Liu, H.; Zhang, X.; Zhang, P.; Zhu, Q. Z.; Du, H. L.; Wang, L. L.; Zhang, R. P.; Xu, B. MOF-derived ZnS nanodots/$Ti_3C_2T_x$ MXene hybrids boosting superior lithium storage performance. *Nano-Micro Lett.* **2021**, *13*, 202.

[91] Shang, Z.; Yu, W. H.; Zhou, J. H.; Zhou, X.; Zeng, Z. Y.; Tursun, R.; Liu, X. G.; Xu, S. M. Recycling of spent lithium-ion batteries in view of graphite recovery: A review. *eTransportation* **2024**, *20*, 100320.

[92] Yang, S. Z.; Gao, Q. Q.; Li, Y. K.; Cai, H. W.; Li, X. D.; Sun, G. X.; Zhuang, S. X.; Tong, Y. J.; Luo, H.; Lu, M. Residual fluoride self-activated effect enabling upgraded utilization of recycled graphite anode. *J. Energy Chem.* **2024**, *93*, 24–31.

[93] Qin, H. Q.; Mo, Z. Z.; Lu, J.; Sui, X.; Song, Z. F.; Chen, B.; Zhang, Y. J.; Zhang, Z. J.; Lei, X. X.; Lu, A. J. et al. Ultrafast transformation of natural graphite into self-supporting graphene as superior anode materials for lithium-ion batteries. *Carbon* **2024**, *216*, 118559.

[94] Cheng, X. B.; Liu, H.; Yuan, H.; Peng, H. J.; Tang, C.; Huang, J. Q.; Zhang, Q. A perspective on sustainable energy materials for lithium batteries. *SusMat* **2021**, *1*, 38–50.

[95] Natarajan, S.; Divya, M. L.; Aravindan, V. Should we recycle the graphite from spent lithium-ion batteries? The untold story of graphite with the importance of recycling. *J. Energy Chem.* **2022**, *71*, 351–369.

[96] Liu, J. J.; Shi, H.; Yu, K.; Geng, Y. N.; Hu, X. Y.; Yi, G. P.; Zhang, J. Z.; Luo, X. B. Regeneration and reuse of anode graphite from spent lithium-ion batteries with low greenhouse gas (GHG) emissions. *Chin. Chem. Lett.* **2023**, *34*, 108274.

[97] Dong, S.; Song, Y. L.; Ye, K.; Yan, J.; Wang, G. L.; Zhu, K.; Cao, D. X. Ultra-fast, low-cost, and green regeneration of graphite anode using flash joule heating method. *EcoMat* **2022**, *4*, e12212.

[98] Qiao, Y.; Zhao, H. P.; Shen, Y. L.; Li, L. Q.; Rao, Z. H.; Shao, G. S.; Lei, Y. Recycling of graphite anode from spent lithium-ion batteries: Advances and perspectives. *EcoMat* **2023**, *5*, e12321.

[99] Wang, J. R.; Yang, D. H.; Xu, Y. J.; Hou, X. L.; Ang, E. H.; Wang, D. Z.; Zhang, L.; Zhu, Z. D.; Feng, X. Y.; Song, X. H. et al. Recent developments and the future of the recycling of spent graphite for energy storage applications. *New Carbon Mater.* **2023**, *38*, 787–803.

[100] Chen, W.; Qu, H. T.; Shi, R. Y.; Wang, J. X.; Ji, H. C.; Zhuang, Z. F.; Ma, J.; Tang, D.; Li, J. F.; Tang, J. et al. Upcycling spent graphite into fast-charging anode materials through interface regulation. *ACS Energy Lett.* **2024**, *9*, 3505–3515.

[101] Shi, Z. Y.; Wang, S. L.; Jin, Y. H.; Zhao, L. F.; Chen, S. W.; Yang, H. M.; Cui, Y. X.; Svanberg, R.; Tang, C. C.; Jiang, J. C. et al. Establishment of green graphite industry: Graphite from biomass and its various applications. *SusMat* **2023**, *3*, 402–415.

[102] Ko, M.; Chae, S.; Ma, J.; Kim, N.; Lee, H. W.; Cui, Y.; Cho, J. Scalable synthesis of silicon-nanolayer-embedded graphite for high-

energy lithium-ion batteries. *Nat. Energy* **2016**, *1*, 16113.

[103] Li, H. D.; Li, H. Y.; Lai, Y. Z.; Yang, Z. W.; Yang, Q.; Liu, Y. X.; Zheng, Z.; Liu, Y. X.; Sun, Y.; Zhong, B. H. et al. Revisiting the preparation progress of nano-structured Si anodes toward industrial application from the perspective of cost and scalability. *Adv. Energy Mater.* **2022**, *12*, 2102181.

[104] Zhai, Y.; Zhong, Z. T.; Kuang, N. N.; Li, Q.; Xu, T. Z.; He, J. X.; Li, H. M.; Yin, X. J.; Jia, Y. R.; He, Q. et al. Both resilience and adhesivity define solid electrolyte interphases for a high performance anode. *J. Am. Chem. Soc.* **2024**, *146*, 15209–15218.

[105] Zhang, R.; Chen, X.; Shen, X.; Zhang, X. Q.; Chen, X. R.; Cheng, X. B.; Yan, C.; Zhao, C. Z.; Zhang, Q. Coralloid carbon fiber-based composite lithium anode for robust lithium metal batteries. *Joule* **2018**, *2*, 764–777.

[106] Shen, X.; Cheng, X. B.; Shi, P.; Huang, J. Q.; Zhang, X. Q.; Yan, C.; Li, T.; Zhang, Q. Lithium-matrix composite anode protected by a solid electrolyte layer for stable lithium metal batteries. *J. Energy Chem.* **2019**, *37*, 29–34.

[107] Lee, Y. G.; Fujiki, S.; Jung, C.; Suzuki, N.; Yashiro, N.; Omoda, R.; Ko, D. S.; Shiratsuchi, T.; Sugimoto, T.; Ryu, S. et al. High-energy long-cycling all-solid-state lithium metal batteries enabled by silver-carbon composite anodes. *Nat. Energy* **2020**, *5*, 299–308.

[108] Gao, Y. C.; Yao, N.; Chen, X.; Yu, L. G.; Zhang, R.; Zhang, Q. Data-driven insight into the reductive stability of ion-solvent complexes in lithium battery electrolytes. *J. Am. Chem. Soc.* **2023**, *145*, 23764–23770.

Acknowledgements

This work was supported by the National Key R&D Program of China (2022YFB2404402), S&T Program of Hebei (22344402D), National Natural Science Foundation of China (T2322015, 22393900, and 22109086), the Beijing Natural Science Foundation (L233004), the Seed Fund of Shanxi Research Institute for Clean Energy, the Tsinghua University Initiative Scientific Research Program, and Ordos Laboratory.

Author contributions

B.C., M.D., Z.G., H.L., C.Y., A.C., and X.C. prepared the initial manuscript. C.T., J.-Q.H. and Q.Z. revised the manuscript. All authors have given approval to the final version of the manuscript.

Competing interests

The authors declare no competing interests.

Additional information

This is an article in honor of Professor Yong Jin on his 90th birthday.